DOI: 10.1002/fuce.200900056

Carbon Nanotubes Based Nafion Composite Membranes for Fuel Cell Applications

N. P. Cele[1,2], S. Sinha Ray[1]*, S. K. Pillai[1], M. Ndwandwe[2], S. Nonjola[3], L. Sikhwivhilu[1], and M. K. Mathe[3]

[1] DST/CSIR Nanotechnology Innovation Centre, National Centre for Nano-Structured Materials, Council for Scientific and Industrial Research, 1-Meiring Naude Road, Brummeria, Pretoria 0001, Republic of South Africa
[2] Department of Physics and Engineering, University of Zululand, Kwadlangezwa 3886, Republic of South Africa
[3] Energy and Processes, Material Science and Manufacturing, Council for Scientific and Industrial Research, 1-Meiring Naude Road, Brummeria, Pretoria 0001, Republic of South Africa

Received October 9, 2009; accepted November 23, 2009

Abstract

Carbon nanotubes (CNTs) containing Nafion composite membranes were prepared *via* melt-blending at 250 °C. Using three different types of CNTs such as pure CNTs (pCNTs), oxidised CNTs (oCNTs) and amine functionalised CNTs (fCNTs); the effect of CNTs surface oxidation as well as functionalisation in composite membranes was investigated by focussing on three aspects: thermo-mechanical stability, thermal degradation and proton conductivity. The oCNTs-containing Nafion composite membrane exhibited concurrent improvement in most of the properties as compared to that of pure Nafion or other CNTs-containing Nafion composite membranes.

Keywords: Carbon Nanotubes, Conductivity, Fuel Cell, Nafion, Nanocomposite Membranes, Thermal Properties, Water Uptake

1 Introduction

Hydrocarbon fuels such as coal, oil and natural gas are widely used as power sources. The depletion of hydrocarbon fuels will eventually lead to the power shortage in most countries, especially in South Africa where storage is not sufficient. The disadvantage of these fossil fuels is their toxic emissions into the atmosphere. This has led to an ever-growing need to find cleaner and pollution-free alternative power sources, which will decrease not only the environmental pollution but also the shortage of electrical energy. Fuel cells are one of the promising alternative power sources, with efficiencies of up to 60% [1–5], higher energy densities relative to batteries and the ability to operate on clean fuels while producing no pollutants. They also operate very quietly, reducing noise pollution [6]. The only by-product of the proton exchange membrane (PEM) fuel cell is water, thus completely eliminating all emissions. Because of these advantages, fuel cells are being developed for numerous applications such as automobiles, portable electronic devices, and for mobile and stationary power generation [7–9]. It is widely known that there are still many technical and market-related issues to overcome before fuel cells can become commercially viable technology on a large scale. These challenges include decreasing the fuel cell cost, choosing the appropriate fuel source and infrastructure, and increasing its performance at higher temperatures of about 100 °C [10, 11].■Please note that the references are renumbered in sequential order in the text as well as in the list.■

Research in the area of fuel cells has exponentially grown over the last 20 years [3–12], especially in PEM fuel cells. These are inexpensive to operate and give the highest efficiency compared to other types of fuel cells. They operate at a relatively low temperature of about 80 °C, which makes them ideal to be used in homes and automobile applications. PEM fuel cell uses a polymer membrane as an electrolyte, which conduct protons to the cathode side. The most commonly used polymer for preparation of membrane is Nafion, a per-

[*] *Corresponding author, rsuprakas@csir.co.za*

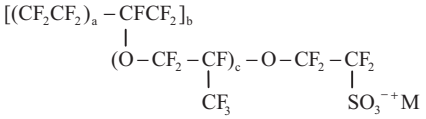

Scheme 1 The molecular structure of Nafion membrane, where a = 6.5–13.5; b = 1, 2, 3. ..; c = 200–1,000 and M^+ is the exchangeable cation.

fluorosulphonyl fluoride copolymer from DuPont. Nafion is the standard by which all new materials are compared. Nafion has also found numerous other applications such as liquid and gas separations, metal ion recovery and the chloro-alkali industry [13]. In the dry state, Nafion is a poor ion conductor, but ionic conductivity increases sharply with water content [9, 11]. Scheme 1 shows the molecular structure of Nafion.

Although Nafion is the most suitable candidate for the fabrication of fuel cell membrane, however, Nafion-based membranes have major drawbacks such as high production cost, low conductivity at low humidity and/or high temperature (>100 °C), loss of mechanical stability at high temperature (~100 °C), elevated MeOH permeability and restricted operation temperature. The higher MeOH/water permeability at high temperatures must be overcome because high MeOH permeability not only decreases the fuel cell efficiency, but also the cathode performance. Furthermore, solid electrolyte membranes with high proton conductivity (>0.01 S cm^{-1}) and little or no dependence on humidity above 100 °C are very desirable, because of the beneficial effect of elevated temperatures on electrode kinetics, carbon monoxide (CO) tolerance of the electrocatalysts and the use of lower amount of precious platinum (Pt) metals [2, 9, 14–17]. One of the most commonly used strategies to overcome these drawbacks is the modification of Nafion by using polymer nanocomposite (PNC) technology.

PNCs have recently shown a worldwide growth effort especially in the fabrication of high temperature PEM for fuel cells [18–21]. In principle, nanocomposites are the extreme case of composites in which the interfacial interactions between two or more phases are maximised to obtain the superior performance as compared to any of the pure solid component. In PNCs, nanometre-size particles of inorganic or organic materials are homogeneously dispersed at a nanoscale level in a polymer matrix [22]. There is a wide variety of nanoparticles, of different natures and sizes that are blended with Nafion to generate new generation materials to improve its properties for PEM fuel cell applications [18–21, 23]. Among them, carbon nanotubes (CNTs) are attracting great research interest as a nanoreinforcing material in PNCs because of their extraordinary high strength and high modulus, their excellent electrical conductivity along with their important thermal conductivity and stability, and their low density [24].

In 2006, Liu et al. [25] tried to fabricate CNTs-containing Nafion membranes by keeping the content of CNTs lower than the percolation threshold. According to them, the mechanical stability of membranes was improved by dispersing 1 wt.% CNTs, without affecting the performances of H_2/O_2 fuel cell. However, the method used for the dispersion of CNTs was a ball-milling followed by solvent casting; this method is not suitable for up-scaling. Thomassin et al. [26] prepared CNTs-based Nafion membrane by a melt-extrusion method in order to decrease the MeOH permeability without deleterious effect on the ionic conductivity. For the preparation of composites, two different types of CNTs were used: commercially available CNTs-containing carboxylic group (abbreviated as commer. CNT–COOH) and CNTs grafted by radicals bearing a 'COOH' group. The tensile modulus of prepared composite increased significantly but there was no report on the thermal degradation and thermo-mechanical stability of the prepared composite membranes.

The main objective of this work is to investigate the effect of CNTs surface functionalisation on the thermal and the thermo-mechanical stability and conductivity of CNTs-based composite membranes. The composite membranes were prepared by a melt-blending-compression-moulding technique. The degree of dispersion of CNTs in the Nafion matrix was studied by scanning electron microscope (SEM). Thermal properties of pure Nafion and composite membranes were studied by both thermogravimetric and dynamic mechanical analysers. The effect of incorporation of CNTs on the direct-current (DC) resistivity and alternating-current (AC) impedance of Nafion membrane are also reported.

2 Experimental

2.1 Materials

The Nafion precursor, i.e. a perfluorosulphonyl fluoride copolymer resin (Nafion R-1100 resin) was purchased from Ion Power, Inc., Bear, DE, USA. More than 95% pure multi-walled carbon nanotubes (from now we will abbreviate multi-walled CNT as CNT) with the outside diameter of 40–60 nm, inside diameter of about 5–10 nm and a length of about 0.5–500 μm, were purchased from Sigma–Aldrich, USA.

2.2 CNTs Surface Oxidation

Pure CNTs (pCNTs) were oxidised by refluxing with 5 M HNO_3 in a ratio of 0.1 g/10 mL for 1 h, followed by filtration (nylon filters 0.45 μm pore size) and washing with deionised water, to remove traces of acid. Oxidised CNTs (oCNTs) were then dried overnight at 110 °C under vacuum.

2.3 CNTs Surface Functionalisation with Hexadecylamine

A mixture of oCNTs (200 mg) and 2 g hexadecylamine (HDA) was refluxed for 4 h at 120 °C. After cooling to room temperature, the excess of HDA was removed by washing with ethanol several times. The solid (i.e. amine functionalised CNTs, fCNTs) was collected by nylon membrane filtra-

tion (0.45 μm pore size) and dried at 110 °C for overnight under vacuum.

2.4 Membrane Preparation

Nafion composite membranes were prepared by melt-mixing the Nafion precursor with CNTs at 250 °C in a Reomix OS (HAAKE) instrument, at a rotor speed of 60 rpm for 10 min. The filler was added after 2 min of melting of Nafion inside the mixer. For each composite, the amount of CNTs loading was fixed to 1 wt.% to avoid short circuiting in fuel cell. Composites were prepared with pure pCNTs, oCNTs and fCNTs (HDA functionalised CNTs), were correspondingly abbreviated as N-pCNTs, N-oCNTs and N-fCNTs, respectively. The dried composite strands were then converted into sheets with a thickness of 0.12–0.2 mm by pressing with 2 MPa pressure at 250 °C for 5 min. The compression moulded sheets were then hydrolysed to have cation exchange properties as follows: compression moulded sheets were immersed in a solution of 15% potassium hydroxide, 50% of deionised water and 35% of dimethyl sulphoxide at 80 °C for 2 h, followed by the repeated immersion (three times) in a fresh 5 M HNO_3 for 1 h.

The membranes were then treated according to the standard procedure by boiling in 5% H_2O_2 (hydrogen peroxide) aqueous solution for 1 h, to remove organic impurities, followed by washing with boiling deionised water for 30 min. The membranes were then boiled in 1 M H_2SO_4 for 1 h to remove inorganic impurities and also to complete protonation before washing with deionised water for 30 min. Washing with deionised water was repeated several times to remove any traces of acids, as checked by pH paper. Finally, all membranes were kept in deionised water prior to measurements.

2.5 Characterisation and Property Measurements

Dry membranes were manually fractured after cooling in liquid nitrogen, to expose their cross-section. The morphology of the fractured sample surfaces was analysed using SEM (LEO 1525), operating at an accelerating voltage of 3–10 kV. To avoid charging, sample surface was coated with gold/palladium alloy. The thermogravimetric analysis (TGA) was conducted on a TGA Q500 (TA Instruments) at a heating rate of 10 °C min^{-1} under air, from room temperature to 700 °C. Mechanical properties of pure Nafion and its CNTs-containing composite membranes were studied by a Perkin Elmer DMA 8000 in the dual cantilever bending geometry. The temperature dependence of loss tangent (tan δ, loss modulus/storage modulus) of all samples were measured at a constant frequency of 1 Hz with the strain amplitude of 0.02% from room temperature to 180 °C with a heating rate of 2 °C min^{-1}.

The bulk DC resistivity of various membranes was measured at room temperature using the four-point-collinear probe method [9]. The equidistant tungsten carbide probes have a separation distance(s) and probe radius of 0.127 and 0.005 cm, respectively. The 1 × 1 cm^2 samples were prepared with a thickness of about 0.2 cm. The Keithley 4200-SCS Semiconductor Characterisation System, equipped with a four supply-and-measure unit (SMU) and a pre-amplifier, was used to perform the high precision DC resistivity characterisation by supplying currents ranging from 1 fA to 1 mA with a resolution of 0.1 fA. The AC impedance measurements of pure Nafion and CNTs-containing composite membranes were performed on films with thickness of about 0.1–0.3 mm at 26 °C and 100% relative humidity. Conductivity measurements were performed on membranes using a homemade cell. The cell geometry was chosen based on previously reported experiments to ensure that the membranes resistance dominates the response of the system [27]. The four-point-probe conductivity cell was made of two perplex blocks, with an area of 5 × 5 cm^2 and an open groove on the top one, to keep membranes fully hydrated. Two copper wire electrodes were used to apply current to the ends of the membrane sample, while another pair of electrodes (1 cm apart) was used to measure the voltage drop across the sample. The membrane samples were sandwiched between two blocks that were pressed together by four screws fastened with approximately the same force to ensure good electrode-membrane contact (see Figure 1). The electrochemical cell was connected using a four-point-probe technique at an Auto lab model 4.90006 Potentiostat and Frequency Response Analyser (FRA). The FRA electrochemical impedance software was used for the impedance measurements from 1 MHz to 1 Hz. The amplitude of the AC voltage was 5 mV. The nanocomposite films were completely dried under vacuum at 90 °C for 24 h, weighed (W_{dry}) and then placed in water/MeOH (50/50 v/v) at 25 °C for 24 h. The nanocomposite films were then wiped quickly with filter paper and weighed (W_{wet}). The water/MeOH uptake was then calculated according to Eq. (1).

$$\text{Water/MeOH uptake}\,(\%) = \frac{W_{wet} - W_{dry}}{W_{wet}} \times 100 \qquad (1)$$

3 Results and Discussion

3.1 Studies on CNTs and Composites Morphology

Parts (a), (b) and (c) of Figure 2, respectively, show the SEM images of pCNTs, oCNTs and fCNTs. From figures we

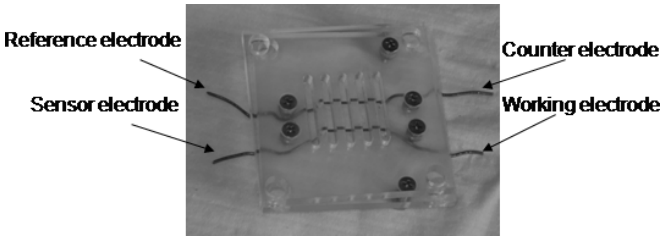

Fig. 1 Four-point-probe cell used for the measurements of proton conductivity.

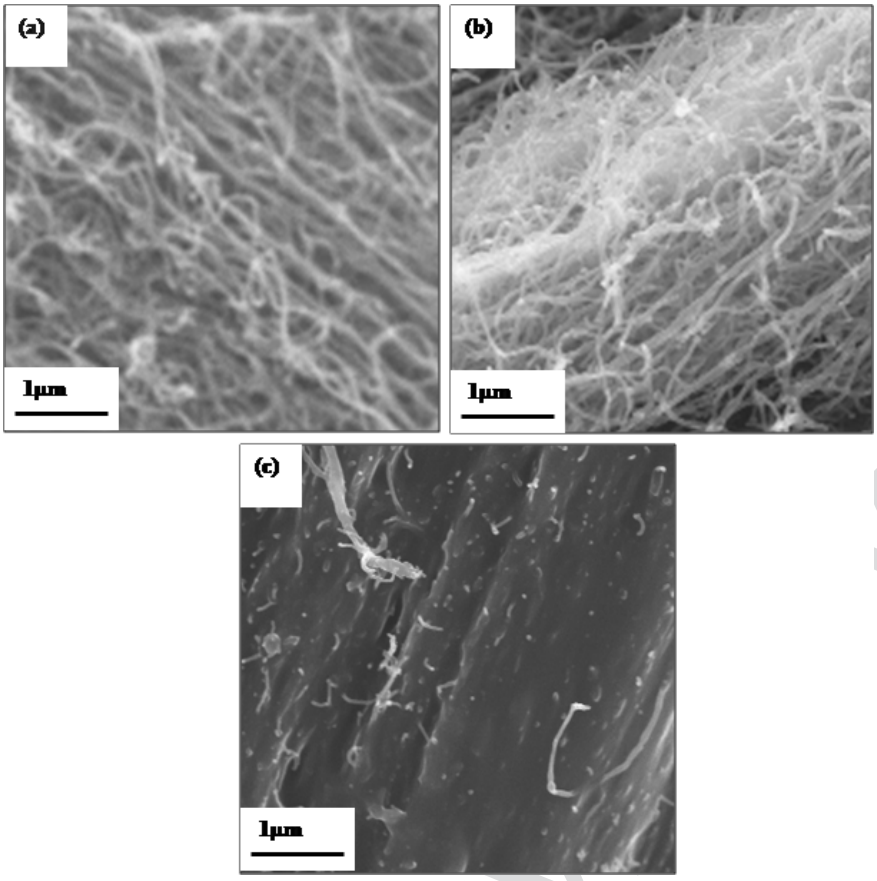

Fig. 2 Field-emission scanning electron microscopy images of (a) pCNTs, (b) oCNTs and (c) fCNTs.

can see pCNTs are loosely bound to one another and aligned in one direction. oCNTs are also loosely bound but randomly distributed. This suggests that carboxylic acid groups promote electrostatic repulsion between the tubes. On the other hand, fCNTs are densely packed, forming big aligned bundles which are fully covered by the HDA chains.

The degree of dispersion of CNTs in the Nafion matrix was studied by SEM. Freeze-fractured surface was used for the morphological studied and results are presented in Figure 3. A good dispersion is observed when pCNTs (see Figure 3a) were incorporated into the Nafion matrix. Although pCNTs are covered with polymer chains, however, homogeneous dispersion of aggregated CNTs is more discernible at a high magnification SEM image (see inset of Figure 3a). Much higher level of dispersion of CNTs with less aggregation into Nafion matrix is obtained when oCNTs were used for composite preparation (see Figure 3b). This can be attributed to the high level of compatibility between the sulphonic acid groups of the Nafion and the COOH groups of oCNTs. Another reason may be due to the less van-der-Waals interactions among the tubes after oxidation, which actually helping tubes to disperse nicely and homogeneously into the Nafion matrix. The poor dispersion of CNTs in the case of fCNTs-containing Nafion composite (Figure 3c) is due to the high degree of covering of CNTs outer surfaces by HDA group, as shown in Figure 2c, where it is not compatible with the Nafion matrix.

3.2 Thermogravimetric Analysis

The TGA scans of pure polymer and composite membranes in air atmosphere are illustrated in Figure 4. It is apparent that the thermal degradation is very similar for all the samples. However, the temperature corresponding to the onset thermal degradation (T_{on}) and the slope of mass loss (%) is different for different composite membranes. The weight losses observed at 30–300 °C pure Nafion, N-pCNTs, N-oCNTs and N-fCNTs membranes are 7.5, 4.2, 2.5 and 3.4%, respectively. This is due to the boundary water loss and this water could not be completely removed at 100 °C. The evaporation temperature of bulk water is higher due to the interaction of water molecules with the sulphonic acid groups of the Nafion resin. The second degradation stage around 380–430 °C is related to the desulphonation process and the third stage around 430–530 °C is associated with the polytetrafluoroethylene (PTFE) backbone decomposition [28–30]. It is clear from TGA scans that the thermal stability of polymer matrix increases after composite formation with CNTs; however, N-oCNTs composite showing higher thermal stability up to 430 °C (see Figure 3b). Similar behaviour in terms of thermal stability of PNCs containing CNTs has been reported in the literature [31, 32]. Furthermore, Marosfoi et al. [33] reported that the thermal stabilisation effect of CNTs could be attributed to the increased interfacial interactions between the CNTs and polymer, which leads to an increase of the thermal degradation activation energy. In the case of N-oCNT composite membrane, because of the strong interfacial interactions between the CNT surface'-COOH' groups and Nafion polymer chains, CNTs are homogeneously dispersed in the Nafion matrix. Such homogeneous dispersion of oCNTs enhances the performance towards thermal stability by increasing the degradation activation energy and also by acting as superior insulator and mass-transport barrier to the volatile products generated during thermal decomposition [34, 35]. On the other hand, the higher thermal stability of N-pCNTs composite in the temperature range of 430–550 °C is due to the presence of pCNT, which by nature has higher thermal stability in the high temperature region compared to oCNT or fCNT, used for this study [36].

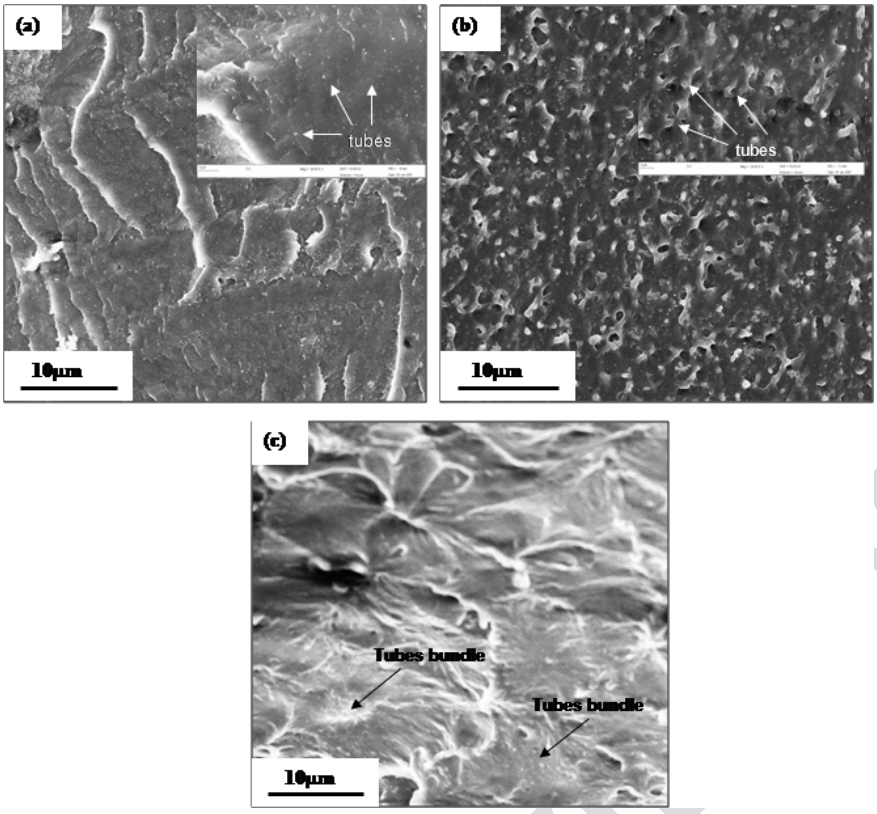

Fig. 3 Field-emission scanning electron microscopy images of freeze-fractured surface of CNTs-containing Nafion composite membranes: (a) N-pCNTs, (b) N-oCNTs and (c) N-fCNTs.

is close to the glass transition temperature (T_g) of the ionic clusters of the Nafion resin [37]. For pure polymer membrane the maximum tan δ or T_g peak appears at about 140 °C; and when pCNTs and oCNTs were incorporated into the Nafion matrix, the T_g of Nafion matrix shifts to the higher temperature range. The highest T_g of about 160 °C is observed in the case of N-oCNTs composite membrane. This confirms that the N-oCNTs composite membrane has an excellent thermo-mechanical stability compared to other membranes. This dramatic improvement in thermo-mechanical stability is due to the homogeneous dispersion of o-CNTs into the Nafion matrix, as a result of the possible strong interaction between the COOH groups on oCNTs outer surfaces and sulphonic groups of Nafion matrix. However, in the case of N-fCNTs composite membrane, the T_g of matrix shifts to the lower temperature region, indicating poor thermo-mechanical stability which is associated with the poor dispersion of fCNTs in the Nafion matrix. Presence of HDA in the composite membrane, which

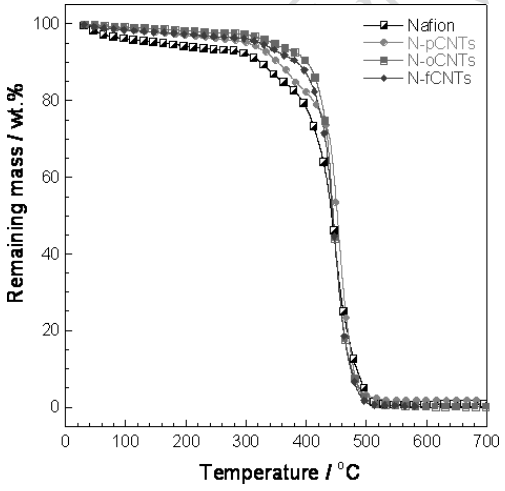

Fig. 4 Thermogravimetric analysis scans of various samples under air atmosphere and heating rate 10 °C min^{-1} from room temperature to 700 °C.

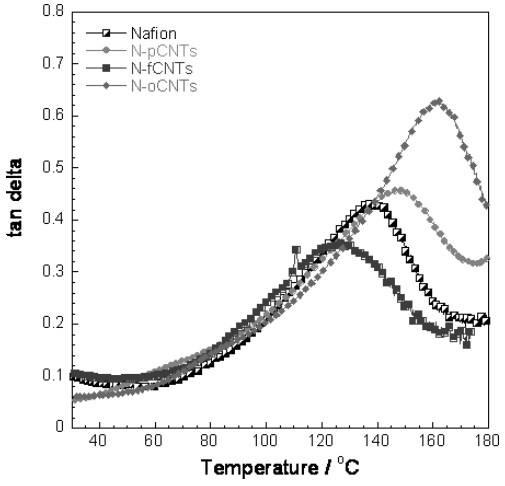

Fig 5 Temperature dependence of tan δ (loss modulus/storage modulus) of the pure Nafion and its CNTs-containing composite membranes.

3.3 Mechanical Properties

DMA results in Figure 5 show the temperature dependence of tan δ curve of the pure Nafion resin and various CNTs-containing composite membranes. There is only one peak observed in the temperature range examined here (25–180 °C). This peak is attributed to the a-relaxation which acts as a plasticiser for Nafion matrix, can be another reason for the observed T_g shift.

3.4 Bulk DC Electrical Resistivity Measurements

The DC electrical resistance of the membranes was measured using a four-point-probe method. The current (I) was

supplied in a range of 1 mA–1 μA through the two outer probes and the voltage drop (V) was measured by the inner probes. The resistance changes as a function of probe spacing (0.127 cm) and is given in Eq. (2).

$$\rho = 2\mathrm{II}s\left(\frac{V}{I}\right) \quad \text{for } t\rangle\rangle s \tag{2}$$

where t is the thickness of the films [19]. The conductivity is then given in Eq. (3).

$$\sigma = \frac{1}{\rho} \tag{3}$$

The resistivity and conductivity values of various membranes are presented in Table 1. The conductivities of N-pCNT and N-oCNT composite membranes are in the range of 10^{-4} S cm^{-1}, which is 1,000 times higher than that of pure Nafion and N-fCNT composite membranes. This could be due to the excellent electrical properties of CNTs and not advantageous for fuel cell application because for fuel application the DC electrical conductivity should be as low as possible.

Table 1 Electrical conductivity measurements of Nafion and its CNT nanocomposites.

Sample	I[a] (A)	R[b] (Ω)	σ[c] (S cm^{-1})
Nafion	10×10^{-6}	10^6	10^{-7}
N-pCNTs	10×10^{-3}	10^3	10^{-4}
N-oCNTs	1.0×10^{-3}	10^3	10^{-4}
N-fCNTs	10×10^{-6}	10^6	10^{-7}

a) Current supplied through the two outer probes.
b) Resistance calculated from the voltage drop measured by inner probes and supplied current.
c) Electrical conductivity range calculated using Eq. (3).

3.5 Proton Conductivity

In order to understand the proton conductivity of prepared composite membranes, electrochemical impedance spectroscopy (EIS) analysis was performed. The impedance plots (Nyquist plots) and Bode plots for pure polymer and composite membranes are shown in Figures 6 and 7, respectively. The experimental data was fitted to the equivalent circuits $R1$(C[$R2$W]) for the pure Nafion resin, N-pCNTs and N-oCNTs composite membranes, whereas N-fCNTs composite membrane was fitted with $R1$($R2$C) circuit. The electrolyte resistance ($R1$) was estimated from fitting procedure and proton conductivity of membranes was then calculated using Eq. (4).

$$\sigma = \frac{d}{RA} \tag{4}$$

where d is the distance between electrodes, R is the bulk resistance and A is the cross-sectional area of the membrane (thickness × length, cm^2). The active length for all membranes was 3 cm. The fitting parameters and conductivity values are tabulated in Table 2.

In Nyquist plots (Z'' *versus* Z'), where Z'' = imaginary part of impedance and Z' = real part of impedance, frequencies

Table 2 Parameters for circuit elements evaluated by fitting data to the equivalent circuit and calculated conductivity for prepared composite membranes.

Sample	Water/MeOH uptake (%)	Slope of Z[a] *versus* log f[b]	t[c] (cm)	σ[d] (S cm^{-1})	$\Delta(C)^{e)}/\Delta(P)^{f)}$
Nafion	22.0	0.3	2.0×10^{-2}	2.04×10^{-4}	7.5×10^{-2}
N-pCNTs	9.5	0.2	3.0×10^{-2}	2.45×10^{-4}	4.5×10^{-2}
N-oCNTs	6.5	0.157	2.3×10^{-2}	1.01×10^{-4}	3.8×10^{-2}
N-fCNTs	8.0	0.001	1.5×10^{-2}	3.02×10^{-5}	1.8×10^{-2}

The average calculated error is about 8%.
a) Absolute impedance.
b) Frequency.
c) Thickness of the membrane.
d) Proton conductivity of nanocomposites membranes.

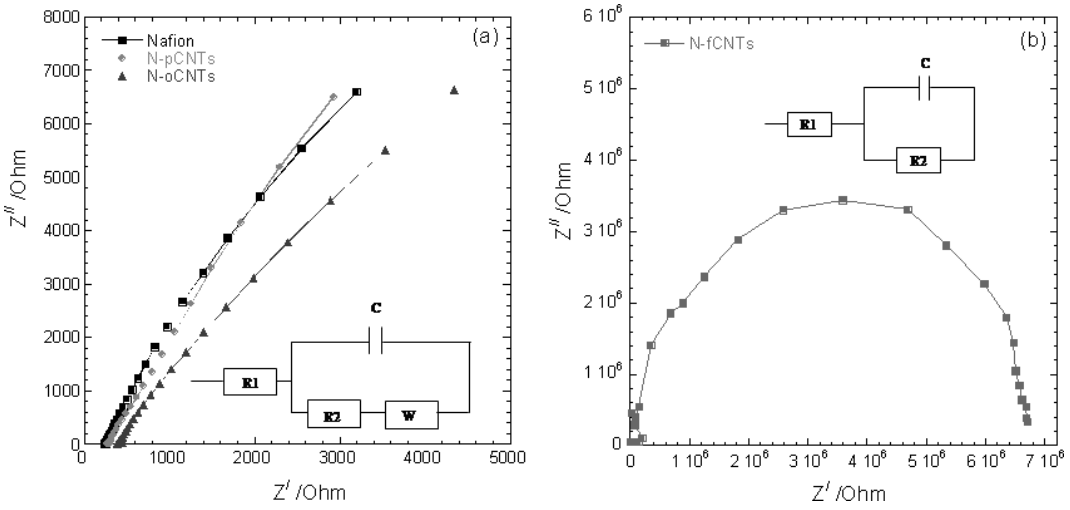

Fig. 6 Nyquist impedance plots and their equivalent circuits for: (a) pure Nafion membrane and N-pCNT and N-oCNTs composite membranes; (b) N-fCNTs composite membranes measured at room temperature.

decrease from the left to the right. The frequency range at which either the semicircle or straight line is observed depends strongly on the ionic conductivity of the material. For pure Nafion, N-pCNTs and N-oCNTs composite membranes, impedance appears as a straight line. This is called Warburg impedance, which is associated with the Warburg infinite behaviour at an electrolytes interface [38] and this depends on the thickness of a material. For N-fCNTs composite membrane, a semicircular arc is observed. This is attributed to the bulk properties of mixed kinetics and diffusion control of a material. The diameter of a semicircle is about 6.5 M Ω, which is equal to the charge transfer resistance (*R*2). The electrolyte resistance (*R*1) strongly influence proton conductivity and can be obtained by extrapolation at the high frequency intercept. A slight increase in electrolyte resistance is observed when CNTs were incorporated into the Nafion matrix, indicative of a decrease in ionic conduction. However, the poorest ionic conduction is observed with N-fCNTs composite membrane. This might be due to the presence of amine functional surfactant chains on the tubes' outer surfaces which hinder the ionic conduction through the composite membranes. The poor dispersion of fCNTs in the Nafion matrix also contributes to the very low ionic conductivity of N-fCNTs-containing composite membrane. The same data was plotted in Bode format (see Figure 7). The phase angle at lower frequencies approaches to 65° for pure Nafion, N-pCNT and N-oCNT composite membranes, whereas phase angle approaches to 75° for N-fCNTs composite membrane, indicative of mixed kinetics and adsorption processes. The slope of *Z versus* log *f* plots indicates the pseudo-capacitive behaviour, which is a good indication of ionic transfer through the membranes.

The water uptake in PEM fuel cell is essential as membrane hydration, required for high proton conductivity. However, the uptake of both water and MeOH must be as low as possible to avoid the flooding and poisoning of the catalyst layer.

4 Conclusion

In summary, CNTs-containing Nafion composite membranes were fabricated using a melt-mixing-compression-moulding process. Thermal stability of all composite membranes was improved with the addition of only 1 wt.% of CNTs. The Nafion composite membrane containing 1 wt.% of oCNTs shows dramatic improvement in thermo-mechanical stability compared to the pure Nafion and other composite

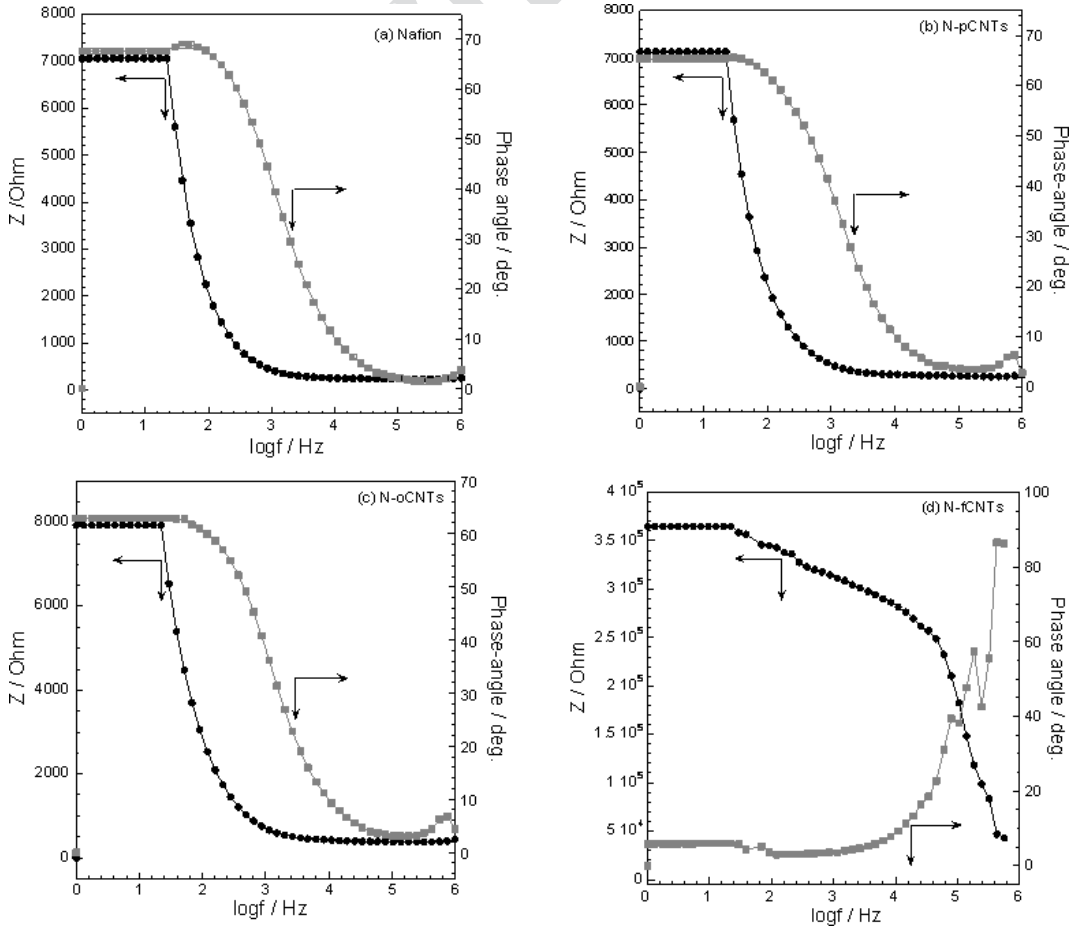

Fig. 7 Bode plots of impedance spectra of pure Nafion and three different composite membranes.

membranes. This is due to the high level of compatibility between the oCNTs outer surfaces and the Nafion matrix. The DC electrical conductivity of the Nafion-based composites was improved when pCNTs was used as filler. The proton conductivity decreases with the incorporation of CNTs. Such observations suggest that filler amount must be reduced to maintain a higher resistivity and increase proton conductivity. On the basis of thermal and thermo-mechanical stability and proton conductivity, the oCNTs-containing Nafion composite membrane will be the best membrane for fuel cell applications. Further investigation to optimise the oCNTs concentration in the Nafion matrix and to get a membrane with a balance of all properties is in progress in our laboratory.

Acknowledgements

Authors from the National Centre for Nano-Structured Materials acknowledge the CSIR Executive and the Department of Science and Technology, South Africa for financial support.

References

[1] H.-F. Cui, J.-S. Ye, W.-D. Zhang, J. Wang, F.-S. Sheu, *J. Electroanal. Chem.* **2005**, *577*, 295.
[2] M. Watanabe, H. Uchida, Y. Seki, M. Emori, *J. Electrochem. Soc.* **1996**, *143*, 3847.
[3] G. Cacciola, V. Antonucci, S. Freni, *J. Power Sources* **2001**, *100, 67.*
[4] R. F. Silva, S. Passerini, A. Pozio, *Electrochim. Acta* **2005**, *50*, 2639.
[5] X. Ren, P. Zelenay, S. Thomas, J. Davey, S. Gottesfeld, V. Plzak, B. Rohland, *J. Power Sources* **2001**, *86*, 111.
[6] K. V. Kordesch, G. R. Simander, *Chem. Rev.* **1995**, *95*, 191.
[7] C. Heitner-Wirguin, *J. Membr. Sci.* **1996**, *120*, 1.
[8] A. V. Anantaraman, C. L. Gardner, *J. Electroanal. Chem.* **1996**, *414*, 115A.
[9] P. Jannasch, *Curr. Opin. Colloid Interface Sci.* **2003**, *8*, 96.
[10] M. F. Mathias, J. Roth, J. Fleming, W. Lehnert, in *Handbook of Fuel Cells, Fundamentals, Technology and Applications, Vol. 3* (Eds. W. Vielstich, A. Lamm, H. A. Gastegier), WILEY-5, **2003**, pp. 517.■Please provide the publisher location.■
[11] M. Doyle, G. Rajendran, in *Handbook of Fuels Cell Fundamentals* (Ed. W. Vielstich), WILEY-3, **2003**, pp. 351. ■Please provide the publisher location.■
[12] F. Barbir, S. Yazici, *Int. J. Energy Res.* **2008**, *32*, 369.
[13] R. B. Gunn, F. Peter, R. A. Curran, *Biophys. J.* **1971**, *11*, 559.
[14] M. Watanabe, Y. Seki, M. Emori, *J. Phys. Chem.* **1998**, *B102*, 3129.
[15] E. Chida, Y. Seki, L. Agihara, M. Watanabe, *Electrochem. Soc.* **2003**, *150*, 957.
[16] J.-M. Thomassin, C. Pagnoulle, D. Bizzari, G. Caldarella, A. Germain, R. Jerome, *e-Polymers* **2004**, *18*, 19.
[17] D. H. Jung, S. Y. Cho, D. H. Peck, D. R. Shin, J. S. Kim, *J. Power Sources* **2003**, *118*, 205.
[18] Y. Deyrail, F. Mighri, M. Bousmina, S. Kaliaguine, *Fuel Cells* **2007**, *6*, 447.
[19] D. H. Jung, S. Y. Cho, D. H. Peck, D. R. Shin, J. S. Kim, *J. Power Sources* **2003**, *118*, 205.
[20] B. Pascal, A. B. Allen, C. Peter, W. Andy, *J. Mater. Chem.* **2003**, *13*, 2540.
[21] S. Bouatia, F. Mighri, M. Bousmina, *Fuel Cells* **2008**, *2*, 120.
[22] S. Sinha Ray, M. Okamoto, *Prog. Polym. Sci.* **2003**, *28*, 1529.
[23] H. Xu, K. Chen, X. Guo, J. Fang, J. Yin, *J. Membr. Sci.* **2007**, *288*, 255.
[24] S. Sinha Ray, S. Vaudreuil, A. Maazouz, M. Bousmina, *J. Nanosci. Nanotechnol.* **2006**, *6*, 2191.
[25] Y. H. Liu, B. Yi, Z. G. Shao, D. Xing, H. Zhang, *Electrochem. Solid-State Lett.* **2006**, *9*, 356.
[26] J. M. Thomassin, J. Kollar, G. Caldarella, A. Germain, R. Jerome, C. Detrembleur, *J. Membr. Sci.* **2007**, *303*, 252.
[27] P. Mukoma, B. R. Jooste, H. C. M. Vosloo, *J. Power Sources* **2004**, *136*, 16.
[28] Q. Deng, C. A. Wilkie, R. B. Moore, K. A. Mauritz, *Polymer* **1998**, *39*, 5961.
[29] F. J. Fernandez-Carretero, V. Compan, E. Riande, *J. Power Sources* **2007**, *173*, 68.
[30] H. S. Park, Y. J. Kim, W. H. Hong, Y. S. Choi, H. K. Lee, *Macromolecules* **2005**, *38*, 2289.
[31] M. Zanetti, G. Camino, P. Reichert, R. Mulhaupt, *Macromol. Rapid Commun.* **2001**, *22*, 176.
[32] Y. Tang, Y. Hu, L. Song, R. Zong, Z. Gui, Z. Chen, *Polym. Degrad. Stab.* **2003**, *82, 127.*
[33] B. B. Marosfoi, A. Szabó, G. Marosi, D. Tabuani, G. Camino, S. Pagliari, *J. Therm. Anal. Calorim.* **2006**, *86*, 669.
[34] X.-L. Xie, Y.-W. Mai, X.-P. Zhou, *Mater. Sci. Eng.* **2005**, *R49*, 89.
[35] T. Kashiwagi, E. Grulke, J. Hilding, R. Harris, W. Awad, J. Douglas, *Macromol. Rapid Commun.* **2002**, *232*, 761.
[36] S. K. Pillai, S. Sinha Ray, M. Moodley, *J. Nanosci. Nanotechnol.* **2008**, *8*, 6187.
[37] F. Bauer, S. Denneler, M. Willert-Porada, *J. Polym. Sci. Part B: Polym. Phys.* **2005**, *43*, 786.
[38] Y. Zhang, Y. Huang, *Solid State Ionics* **2006**, *177*, 65.